ARTICLE IN PRESS

Available online at www.sciencedirect.com

SCIENCE DIRECT®

Journal of Theoretical Biology ▮ (▮▮▮▮) ▮▮▮–▮▮▮

Journal of Theoretical Biology

www.elsevier.com/locate/yjtbi

Transmission dynamics of the great influenza pandemic of 1918 in Geneva, Switzerland: Assessing the effects of hypothetical interventions

G. Chowell[a,*], C.E. Ammon[b,1], N.W. Hengartner[a], J.M. Hyman[a]

[a]*Theoretical Division (MS B284), Los Alamos National Laboratory, Los Alamos, NM 87545, USA*
[b]*Institute of Social and Preventive Medicine, Faculty of Medicine, CMU, P.O. Box 1211, Geneva 4, Switzerland*

Received 31 August 2005; received in revised form 11 November 2005; accepted 14 November 2005

Abstract

Recurrent outbreaks of the avian H5N1 influenza virus in Asia represent a constant global pandemic threat. We characterize and evaluate hypothetical public health measures during the 1918 influenza pandemic in the Canton of Geneva, Switzerland. The transmission rate, the recovery rate, the diagnostic rate, the relative infectiousness of asymptomatic cases, and the proportion of clinical cases are estimated through least-squares fitting of the model to epidemic curve data of the cumulative number of hospital notifications. The latent period and the case fatality proportion are taken from published literature. We determine the variance and identifiability of model parameters via a simulation study. Our epidemic model agrees well with the observed epidemic data. We estimate the basic reproductive number for the spring wave $\hat{\mathcal{R}}_1 = 1.49$ (95% CI: 1.45–1.53) and the reproductive number for the fall wave $\hat{\mathcal{R}}_2 = 3.75$ (95% CI: 3.57–3.93). In addition, we estimate the clinical reporting for these two waves to be 59.7% (95% CI: 55.7–63.7) and 83% (95% CI: 79–87). We surmise that the lower reporting in the first wave can be explained by a lack of initial awareness of the epidemic and the relative higher severity of the symptoms experienced during the fall wave. We found that effective isolation measures in hospital clinics at best would only ensure control with probability 0.87 while reducing the transmission rate by $>76.5\%$ guarantees stopping an epidemic.

Keywords: Spanish flu; Pandemic; Influenza; Reproductive number; Switzerland

1. Introduction

Recurrent outbreaks of avian influenza (H5N1) in Asia threaten the human population with the next influenza pandemic as infections have been observed in humans with probable limited human-to-human transmission. Should the new virus subtype get fully adapted for human-to-human transmission, an influenza pandemic could arise (Snacken, 2002; Enserink, 2005) with devastating economic consequences (Meltzer et al., 1999). Therefore, enhancing our understanding of the transmissibility, mechanisms, and key factors under which the influenza virus propagates among populations is critical to devise effective and economic interventions strategies.

The etiological agent of influenza is an RNA virus (orthomyxoviridae family) (Webster et al., 1992) that causes acute upper respiratory tract infection with symptoms including high fever, myalgia, severe malaise, non-productive cough, and sore throats. The duration of the latent period for influenza is about 1.9 days (Mills et al., 2004) followed by an infectious period of about 4 days (Reeve et al., 1980; Moritz et al., 1980). Influenza is transmitted by direct contact (e.g. hand shaking, sweat, etc.), aerosol, and droplets.

Individuals exposed to the influenza virus gain protection or cross-protection. Hence, the influenza virus undergoes continuous evolution in order for annual epidemics to occur. Such changes in the virus composition are known as drifts or shifts. Drifts are the consequence of single-point mutations in the virus antigenic structure while shifts are major gene reassortments which have the potential of generating pandemics (Webster et al., 1992).

*Corresponding author. Tel.: +1 505 606 1483; fax: +1 505 665 5757.
E-mail address: chowell@lanl.gov (G. Chowell).
[1]Los Alamos Unclassified Report LA-UR-05-7140.

0022-5193/$ - see front matter © 2005 Elsevier Ltd. All rights reserved.
doi:10.1016/j.jtbi.2005.11.026

The 1918 influenza pandemic known as the "Spanish flu" caused by the influenza virus A(H1/N1) has been the worst in recent history with estimated worldwide mortality ranging from 20 to 100 million deaths (Cunha, 2004). The worldwide 1918 influenza pandemic spread in three waves starting from Midwestern United States in the spring of 1918 (Patterson and Pyle, 1991; Johnson and Mueller, 2002). The deadly second wave began in late August probably in France while the third wave is generally considered as part of normal more scattered winter outbreaks similar to those observed after the 1889/90 pandemic (Patterson and Pyle, 1991). Subsequent flu pandemics are attributed to flu A(H2N2) in 1957 (Asian flu) and A(H3N2) in 1968 (Hong Kong flu).

Underreporting due to the disruptions in the public health system during the 1918/9 pandemic complicate the estimation of attack and death rates in many regions (Patterson and Pyle, 1991), e.g. influenza deaths were not recorded in Russia and the data from developing countries suffers from significant underreporting (Patterson and Pyle, 1991). Nevertheless, in some countries mandatory notifications of flu cases by health care practitioners were implemented during the pandemic. Switzerland provides one of the best databases for the analysis of the 1918/9 influenza pandemic because mandatory notification of flu cases was implemented at the federal level from the beginning of the pandemic (Ammon, 2002). However, there was underreporting from mild cases and cases who were refused admission in overcrowded hospital clinics. In addition, there is good demographic information of the Swiss population at the time of the pandemic.

In this paper, we investigate the 1918/9 influenza pandemic in the Canton of Geneva located in the south western corner of Switzerland and surrounded in its majority by France. We model the transmission dynamics of the spring and fall waves of influenza using an epidemic model that accounts for the known underreporting. Some of the model parameters are estimated via least-squares fitting and the resulting parameter estimates are corroborated via a simulation study. From our fitted model, we estimate the basic reproductive number of the spring and the reproductive number of the fall wave to be 1.49 (95% CI: 1.45–1.53) and 3.75 (95% CI: 3.57–3.93), respectively. In addition, we estimate the clinical reporting for these two waves to be 59.7% (95% CI: 55.7–63.7) and 83% (95% CI: 79–87). We surmise that both the lack of initial awareness of the epidemic and the relative higher severity of the symptoms experienced during the fall wave contributed to the lower reporting rate in the first wave. We found that effective isolation measures in hospital clinics at best would only ensure control with probability 0.87 while reducing the transmission rate by $>76.5\%$ guarantees stopping an epidemic.

2. The 1918 flu pandemic in Geneva, Switzerland

The 1918/9 influenza pandemic affected more than 50% of the population in Geneva, Switzerland (Ammon, 2002). The first wave occurred in July 1918 ("spring wave"), the second deadliest wave in October–November 1918 ("fall wave"), and the third wave was observed at the end of 1918 ("winter wave"). The symptoms presented during the second wave were more severe than for the first wave. Moreover, it seems that individuals infected with the flu were subsequently protected to secondary waves of infection. The mortality rate was highest in the age group 21–40 years and higher in males (Ammon, 2001).

Control measures were implemented (Fig. 1) but there's no evidence of their effectiveness because disruptions in the sanitary, medical, private and public sectors were common. Moreover, the social climate was that of insecurity and there were doubts among the population about the effectiveness of the control measures that included school and church closures, prohibition of public events and visits to hospitals, mandatory spraying of disinfectants on the streets, and authorization of burials within 48 h of death.

Statistics from hospitals were published daily throughout the epidemic. However, mild cases that did not warrant medical attention were unlikely to be diagnosed in hospitals. Hence, this is an important factor to account for when modeling the transmission dynamics of influenza. A thorough review of the 1918/9 pandemic influenza in Geneva, Switzerland is given by Ammon (2001).

3. Materials and methods

3.1. Epidemic model

We model the first two waves of the 1918 influenza pandemic in Geneva, Switzerland (Fig. 2) separately using a compartmental epidemic model. The model (Fig. 3) for the transmission dynamics of pandemic influenza classifies individuals as susceptible (S_i), exposed (E_i), clinically ill and infectious (I_i), asymptomatic and partially infectious (A_i), hospitalized and reported (J_i), recovered (R_i), and death (D_i) where $i = 1, 2$ indices the spring and fall waves, respectively. We assume that the birth and natural death rates have common rate μ and that the population is completely susceptible to the first wave of infection. Individuals that recover during the spring wave are assumed protected to the fall wave (Mills et al., 2004), and the numbers of susceptible, recovered, and dead individuals at the end of the first wave are set to be the corresponding initial conditions to model the second influenza wave. The initial numbers of exposed and infectious individuals for the spring and fall waves were estimated through least-squares fitting (see parameter estimation section). Susceptible individuals in contact with the virus progress to the latent class at the rate $\beta_i(I_i(t) + J_i(t) + q_i A_i(t))/N_i(t)$, where β_i is the transmission rate for wave i, and $0 < q_i < 1$ is a reduction factor in the transmissibility of the asymptomatic class (A_i). Since there is no evidence of the effectiveness of interventions, and disruptions in the sanitary and medical sectors were common (Ammon, 2001), hospitalized individuals (J_i) are

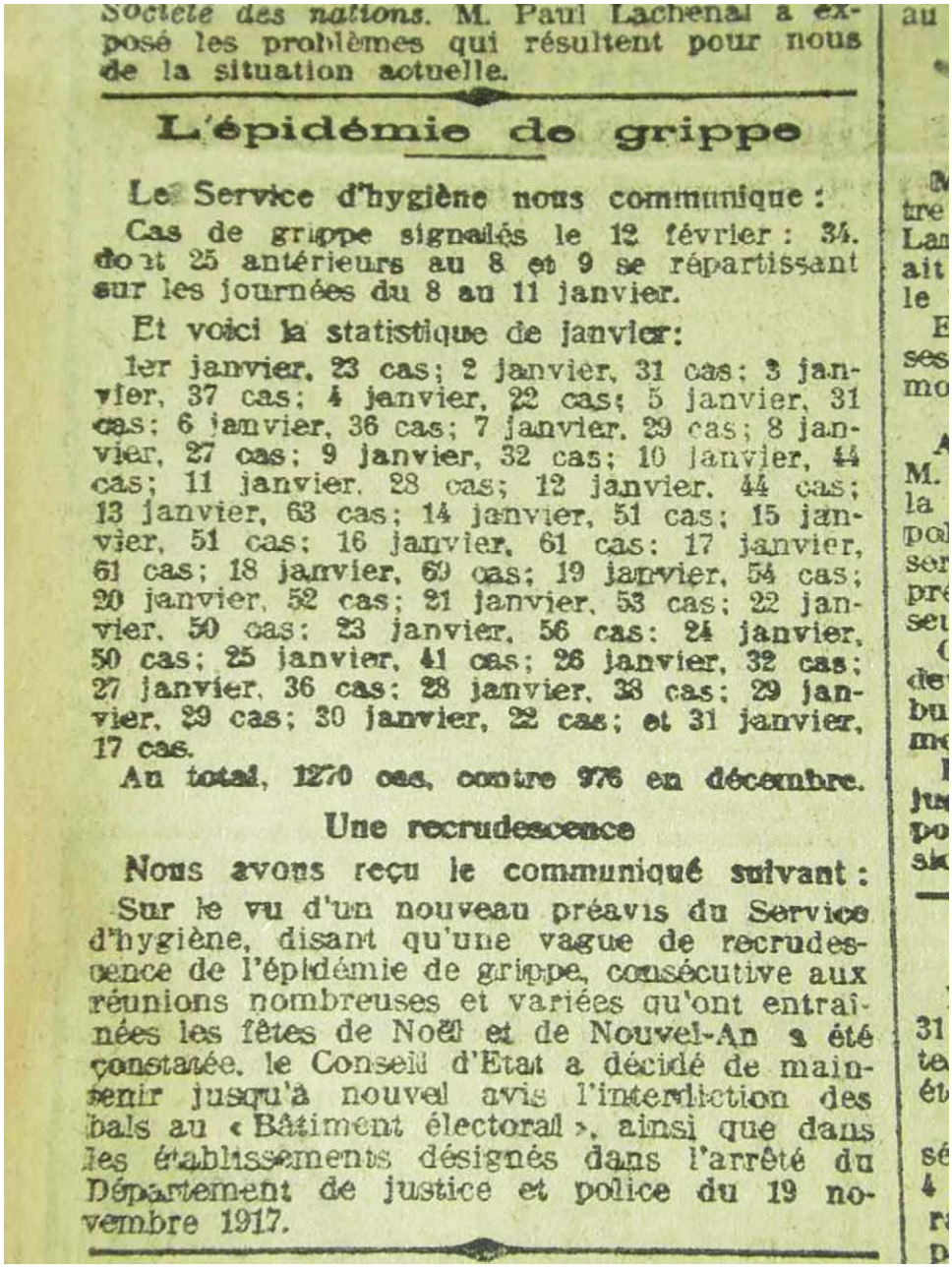

Société des nations. M. Paul Lachenal a exposé les problèmes qui résultent pour nous de la situation actuelle.

L'épidémie de grippe

Le Service d'hygiène nous communique :

Cas de grippe signalés le 12 février : 34, dont 25 antérieurs au 8 et 9 se répartissant sur les journées du 8 au 11 janvier.

Et voici la statistique de janvier:

1er janvier, 23 cas; 2 janvier, 31 cas; 3 janvier, 37 cas; 4 janvier, 22 cas; 5 janvier, 31 cas; 6 janvier, 36 cas; 7 janvier, 29 cas; 8 janvier, 27 cas; 9 janvier, 32 cas; 10 janvier, 44 cas; 11 janvier, 28 cas; 12 janvier, 44 cas; 13 janvier, 63 cas; 14 janvier, 51 cas; 15 janvier, 51 cas; 16 janvier, 61 cas; 17 janvier, 61 cas; 18 janvier, 69 cas; 19 janvier, 54 cas; 20 janvier, 52 cas; 21 janvier, 53 cas; 22 janvier, 50 cas; 23 janvier, 56 cas; 24 janvier, 50 cas; 25 janvier, 41 cas; 26 janvier, 32 cas; 27 janvier, 36 cas; 28 janvier, 38 cas; 29 janvier, 29 cas; 30 janvier, 22 cas; et 31 janvier, 17 cas.

Au total, 1270 cas, contre 976 en décembre.

Une recrudescence

Nous avons reçu le communiqué suivant :

Sur le vu d'un nouveau préavis du Service d'hygiène, disant qu'une vague de recrudescence de l'épidémie de grippe, consécutive aux réunions nombreuses et variées qu'ont entraînées les fêtes de Noël et de Nouvel-An a été constatée, le Conseil d'Etat a décidé de maintenir jusqu'à nouvel avis l'interdiction des bals au « Bâtiment électoral », ainsi que dans les établissements désignés dans l'arrêté du Département de justice et police du 19 novembre 1917.

Fig. 1. An article of the Geneva newspaper La Feuille (no longer active) issued on 02/04/1919 stating statistics of the influenza pandemic and an announcement on the interdiction to organize dancing due to an increase in flu cases after the Christmas and New year celebrations.

assumed infectious. Hence, the total population size at time t for wave i is given by $N_i(t) = S_i(t) + E_i(t) + I_i(t) + A_i(t) + J_i(t) + R_i(t)$. We assumed homogeneous mixing between individuals and, therefore, the fraction $(I_i(t) + J_i(t) + q_i A_i(t))/N_i(t)$ is the probability that a random contact would be with an infectious individual. A proportion $0 < \rho_i < 1$ of latent individuals progress to the clinically infectious class (I_i) at the rate k_i while the rest $(1 - \rho_i)$ progress to the asymptomatic partially infectious class (A_i) at the same rate k_i. Asymptomatic cases progress to the recovered class at the rate γ_{1_i}. Clinically infectious individuals (class I_i) are hospitalized (reported) at the rate α_i or recover without being diagnosed (e.g. mild infections, hospital refusals (Ammon, 2001)) at the rate γ_{1_i}. Hospitalized individuals (reported) recover at the rate $\gamma_{2_i} = 1/(1/\gamma_{1_i} - 1/\alpha_i)$ or die at rate δ_i. The mortality rates were adjusted according to the case fatality proportion (CFP) such that $\delta_i = [CFP/(1 - CFP)](\mu + \gamma_{2_i})$ (see Fig. 3).

The transmission process (for each influenza wave) can be modeled using the following system of nonlinear differential equations:

$$\dot{S}_i(t) = \mu N_i(t) - \beta_i S_i(t)(I_i(t) + J_i(t) + q_i A_i(t))/N_i(t) - \mu S_i(t),$$

$$\dot{E}_i(t) = \beta_i S_i(t)(I_i(t) + J_i(t) + q_i A_i(t))/N_i(t) - (k_i + \mu)E_i(t),$$

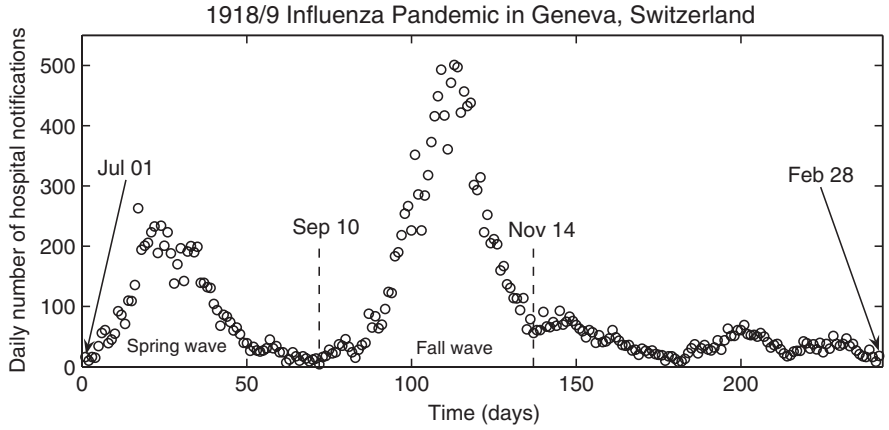

Fig. 2. Daily number of hospital notifications of influenza cases during the 1918/9 influenza pandemic in the Canton of Geneva, Switzerland.

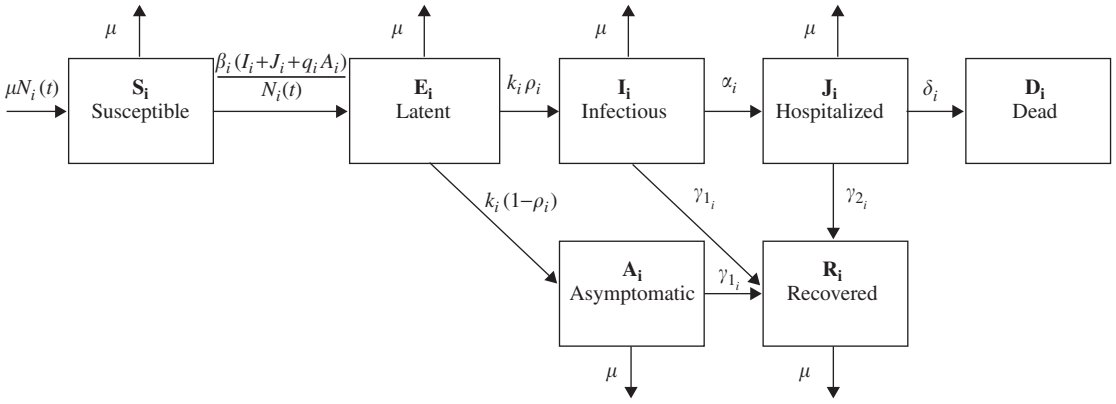

Fig. 3. Flow chart of the state progression of individuals among the different epidemiological classes as modeled by Eq. (1).

$$\dot{A}_i(t) = k_i(1-\rho_i)E_i - (\gamma_{1_i}+\mu)A_i(t),$$

$$\dot{I}_i(t) = k_i\rho_i E_i(t) - (\alpha_i+\gamma_{1_i}+\mu)I_i(t),$$

$$\dot{J}_i(t) = \alpha_i I_i(t) - (\gamma_{2_i}+\delta_i+\mu)J_i(t),$$

$$\dot{R}_i(t) = \gamma_{1_i}(A_i(t)+I_i(t)) + \gamma_{2_i}J_i(t) - \mu R_i(t),$$

$$\dot{D}_i(t) = \delta_i J_i(t),$$

$$\dot{C}_i(t) = \alpha_i I_i(t), \tag{1}$$

where the index $i = 1, 2$ denotes the first ("spring") and second ("fall") waves of infection, respectively. The dot denotes the time derivatives. The cumulative number of hospital notifications, our observed data, is given by $C(t)$.

3.2. The reproductive number

The number of secondary cases generated by a primary infectious case, known as the basic reproductive number $\mathscr{R}_0$ (Anderson and May, 1991; Brauer and Castillo-Chavez, 2000), is a measure of the power of an infectious disease to attack a completely susceptible population. Applying the next-generation method (Diekmann and Heesterbeek, 2000) to our model equations shows that the reproductive number is

$$\mathscr{R}_i = \frac{\beta_i k_i}{k_i+\mu}\left\{\rho_i\left(\frac{1}{\gamma_{1_i}+\alpha_i+\mu} + \frac{\alpha_i}{(\gamma_{1_i}+\alpha_i+\mu)(\gamma_{2_i}+\delta_i+\mu)}\right) + (1-\rho_i)\left(\frac{q_i}{\gamma_{1_i}+\mu}\right)\right\}, \tag{2}$$

where $i = 1, 2$ is used to distinguish the reproductive numbers for the first and second influenza waves of infection, respectively. Notice that $\mathscr{R}_1$ is a basic reproductive number because the population is assumed completely susceptible at the beginning of the epidemic. Also, it can be seen from the above expression that the reproductive number is the sum of the contributions to infection from the different types of infectious individuals namely: infectious but not hospitalized, infectious and hospitalized, and those asymptomatic (partially infectious).

Since the birth and natural death rate μ and the latent period $(1/k_i)$ are known (see Section 3.5), $\gamma_{2_i} = 1/(1/\gamma_{1_i} - 1/\alpha_i)$,

and $\delta_i = [CFP/(1-CFP)](\mu + \gamma_{2_i})$, we can conclude that $\mathscr{R}_i$ is a function of $\{\beta_i, \gamma_{1_i}, \alpha_i, q_i, \text{ and } \rho_i\}$. Estimates of $\mathscr{R}_i$ are obtained from data by substituting the parameter estimates $\hat{\beta}_i, \hat{\gamma_{1_i}}, \hat{\alpha}_i$, $\hat{q}_i$, and $\hat{\rho}_i$ into Eq. (2). The variance of the estimated reproductive number $\mathscr{R}_i$ was obtained from a simulation study (see Parameter estimation).

Reproductive numbers can be used to estimate the magnitude of changes needed to bring an epidemic under control. Because $\mathscr{R}_i$ is a linear function of β_i, the transmission rate per person, if β_i is reduced, then $\mathscr{R}_i$ will also be reduced the same amount. For example, if $\mathscr{R}_i = 4$ and if β_i is reduced by a factor of 4, then $\mathscr{R}_i$ would be reduced to 1. The average transmission rate is a product of the average infectiousness of an infected individual, the susceptibility of the population to infection, and the number of contacts an infected individual has per day. These factors can be reduced by infected people taking precautions to prevent infecting others, susceptible people taking precautions (improved hygiene or vaccinations) to prevent becoming infected, or reducing the number of contacts an infected person has by rapid isolation.

3.3. Clinical reporting

We estimate from our model the extent of reporting of clinical cases (or clinical reporting). This is an important quantity since it also quantifies the extent of under-reporting. Individuals with mild symptoms are unlikely to have sought medical attention, and as a result, would not have been tabulated as flu victims. While these cases are not directly observed, we can estimate the fraction of mild cases from our model. This fraction would include as well individuals that recovered without being properly diagnosed (and hence reported). While misdiagnosis may be common for annual epidemics of influenza due to the limited reliability of clinical diagnosis (non-specific symptoms), clinical diagnosis for the case of pandemic influenza should have been more reliable because of the severity of symptoms particularly during the second wave (Ammon, 2001). The fraction of severe cases that required medical attention is:

$$O_i = \frac{\alpha_i}{\alpha_i + \gamma_{1_i} + \mu}. \tag{3}$$

Similarly an estimate of the amount of clinical under-notification is given by

$$U_i = \frac{\gamma_{1_i}}{\alpha_i + \gamma_{1_i} + \mu}. \tag{4}$$

An estimate of the variance of this quantities was obtained via a simulation study as explained in the parameter estimation section.

3.4. Demographic and epidemic data

The Canton of Geneva is located in the south western corner of Switzerland and covers an area of 282 km^2. The population size of the Canton of Geneva in 1917 was 174 673 which is about 42% of today's population (Dubois, 2005) while the life expectancy was about 60 years ($\hat{\mu} = 1/60\,\text{years}^{-1} = 1/(60*365)\,\text{days}^{-1}$) (Robine and Paccaud, 2005). Daily epidemic data for the Canton of Geneva was obtained from the mandatory notifications registry in Switzerland (Ammon, 2002) during the period July 1918–February 1919 (Fig. 2). The morbidity of the spanish flu in Geneva was 21754 cases (12.45% of total population) with an overall case fatality proportion of 4.2% (Ammon, 2002). Nevertheless, the second influenza wave is well documented to have been much deadlier than the first wave (Ammon, 2002). Because the estimate of the case fatality proportion from Geneva was derived from both waves and was similar to that found by Gani et al. (2005), we chose to use the independent estimates obtained for the first (0.7%) and second (3.25%) waves as reported by Gani et al. (2005).

3.5. Parameter estimation

In our model, we fix the birth and natural death rates to $\hat{\mu} = 1/(60*365)\,\text{days}^{-1}$, and the latent period was fixed to $1/\hat{k_1} = 1/\hat{k_2} = 1.9$ days (Mills et al., 2004). The transmission rate β_i, the recovery rate γ_i, the diagnostic rate α_i, the relative infectiousness of asymptomatic cases q_i, the proportion of clinical cases ρ_i, and the initial numbers of exposed $E_i(0)$ and infectious $I_i(0)$ individuals were estimated through least-squares fitting of $C(t, \mathbf{\Theta}_i)$ in Model (1) ($\mathbf{\Theta}_i$ is the vector of fitting parameters for wave i) to the cumulative number of influenza cases over time y_t (where t denotes time in days) (Fig. 2). The advantage of using the cumulative over the daily number of new cases is that the former somewhat smoothes out known reporting delays on weekends and national holidays. To ensure that the global minimum of this nonlinear regression model is achieved, we repeated the optimization 10 times starting at randomly drawn parameter values from appropriate parameter ranges ($0<\beta_i<50$, $0<\gamma_i<1$, $0<\alpha_i<2$, $0<q_i<1$, $0<\rho_i<1$, $0<E_i(0)<300$, $0<I_i(0)<300$). For the least-squares fitting procedure, we used the Levenberg–Marquardt method with line-search implemented in MATLAB (The Mathworks, Inc.) in the built-in routine `lsqcurvefit` which is part of the optimization toolbox. The resulting parameter estimates are listed in Table 1, and the best model fit to the data is shown in Fig. 4.

The standard deviation of the parameters was obtained from a simulation study using the parametric bootstrap (Efron and Tibshirani, 1986) as follows: The best fit of the cumulative number of reported cases $C(t, \hat{\mathbf{\Theta}}_i)$ to the data was perturbed by simulating alternate realizations. To the best-fit curve $C(t, \hat{\mathbf{\Theta}}_i)$ was added a simulated error structure computed using the increment in the "true" $C(t, \hat{\mathbf{\Theta}}_i)$ from day j to day $j+1$ as the Poisson mean for the number of new case notifications observed in the j to $j+1$ interval. The parameter estimation procedure (described above) was then applied for each of the 1000 simulated realizations.

Table 1
Parameter definitions and baseline estimates for the spring and fall waves of the 1918/9 influenza pandemic in Geneva, Switzerland (Fig. 4)

Parameter	Definition	Source	Spring wave		Fall wave	
			Estimate	S.D.	Estimate	S.D.
β	Transmission rate (days^{-1})	LS	8.00	0.13	5.75	0.24
γ_1	Recovery rate (days^{-1})	LS	0.34	0.01	0.45	0.04
α	Diagnostic rate (days^{-1})	LS	0.51	0.04	2.14	0.11
q	Relative infectiousness of the asymptomatic class	LS	0.003	0.004	0.014	0.01
ρ	Proportion of clinical infections ([0, 1])	LS	0.10	0.01	0.36	0.02
γ_2	Recovery rate for hospitalized class (days^{-1})	—	1.10	0.26	0.58	0.07
δ	Mortality rate (days^{-1})	Gani et al. (2005)	0.01	0.002	0.02	0.002
k	Rate of progression to infectious (days^{-1})	Mills et al. (2004)	0.53	—	0.53	—
μ	Birth and natural death rate (days^{-1})	Robine and Paccaud (2005)	$1/(60*365)$	—	$1/(60*365)$	—
$E(0)$	Initial number of exposed individuals	LS	207	7	9	11
$I(0)$	Initial number of infectious individuals	LS	132	4	34	4

Parameters β_i, γ_i, α_i, q_i, ρ_i, and the initial numbers of exposed and infectious individuals were estimated through least-squares (LS) fitting of the model to the cumulative number of hospital notifications. Parameters k_i, and μ were fixed to baseline estimates obtained from published literature while the mortality rates (δ_i) were estimated from the case fatality proportions as explained in the text. The recovery rate of hospitalized cases $\gamma_{2_i} = 1/(1/\gamma_{1_i} - 1/\alpha_i)$. The standard deviation of the model parameter estimates were obtained from our simulation study using the parametric bootstrap that consisted of 1000 realizations as explained in the parameter estimation section.

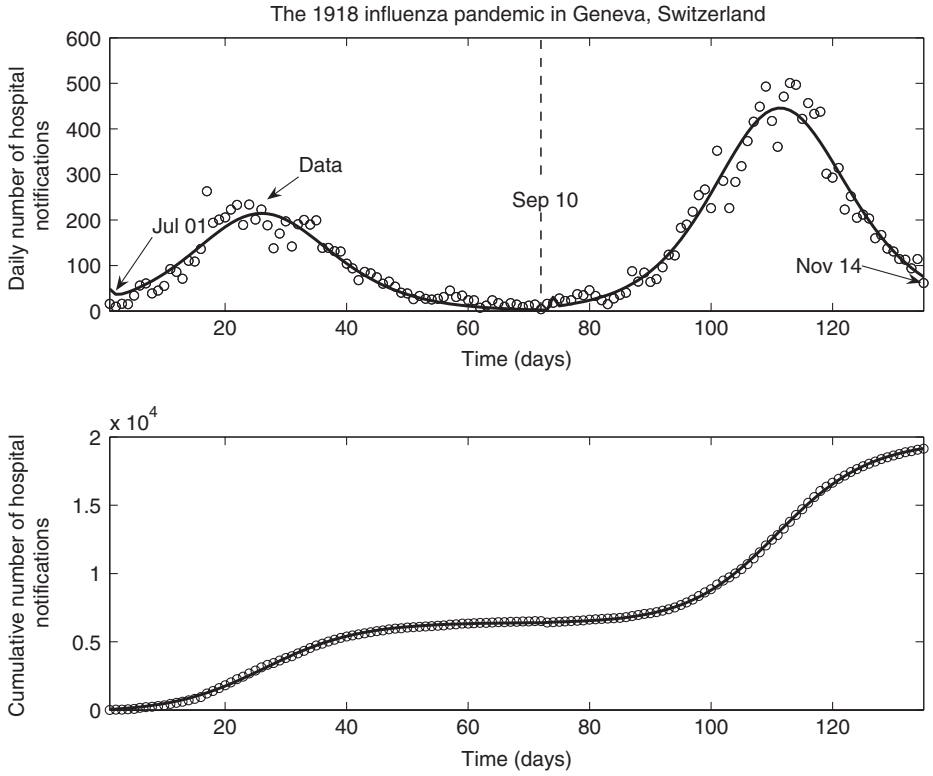

Fig. 4. The best-fit solution obtained by fitting $C(t, \Theta)$ (solid line) in model (1) to the cumulative number of hospital notifications of the spring and fall waves of the 1918 influenza pandemic in Geneva, Switzerland.

This error structure captures the higher variability in the cumulative number of cases observed on the middle course of the epidemic and the smaller variability observed at its beginning and end.

This simulation study allowed us to explore the identifiability of model parameters. Lack of identifiability can be recognized when large perturbations in the model parameters generate small changes in the model output (Pillonetto et al., 2003). A sensitivity analysis can detect non-identifiability of model parameters. Our results indicate that our parameter estimates are stable to perturbations around the model output.

3.6. Modeling intervention strategies

Suppose that hypothetical intervention strategies were prepared and put in place during the "herald" spring wave so that their effects can be quantified on the coming more severe fall wave.

We model the effects of two types of intervention strategies. The first type of strategies have the objective of reducing the probability of transmission per contact (Pourbohloul et al., 2005) through prophylaxis of high-risk groups using antiviral drugs, use of protective devises (e.g. face masks), increase hand washing, and vaccination albeit it is unlikely that enough vaccines would be available in time for an influenza pandemic as the annual vaccine production for inter-epidemic periods currently takes at least 6 months (Webby and Webster, 2003). The second type of strategies are put in place to reduce nosocomial transmission during the pandemic through the implementation of effective isolation strategies in hospital wards.

The first type of interventions reduced the probability of transmission per contact by a factor $0<p<1$, e.g. a 50% reduction in the probability of transmission per contact would be modeled as $p=1/2$. Similarly, the effects of isolation of infectious individuals reduces the transmissibility of hospitalized individuals by a factor $0<\ell<1$ as in Chowell et al. (2003, 2004). We quantify the single and combined impact of these intervention strategies on the reproductive number of the second (fall) wave. The reproductive number $\mathscr{R}_c$ for the second wave that accounts for the above mentioned control strategies is given by

$$\mathscr{R}_c = \frac{\beta_2 p k_2}{k_2+\mu} \times\left\{\rho_2\left(\frac{1}{\gamma_{1_2}+\alpha_2+\mu}+\frac{\ell\alpha_2}{(\gamma_{1_2}+\alpha_2+\mu)(\gamma_{2_2}+\delta_2+\mu)}\right) +(1-\rho_2)\left(\frac{q_2}{\gamma_{1_2}+\mu}\right)\right\}. \quad (5)$$

That is, $\mathscr{R}_c(p=0,\ell=0)=\mathscr{R}_2$.

4. Results

Our fitted model for the influenza notifications during the first two waves of the 1918 influenza pandemic in Geneva, Switzerland agrees well with the observed epidemic data (coefficient of determination of 0.99 (Neter and Wasserman, 1974), Fig. 4).

We estimated epidemiological parameters via least-squares fitting of the model to the cumulative number of hospital notifications (Table 1). We estimated the standard deviations of the parameters via a simulation study using the parametric bootstrap (Fig. 5) and then obtained estimates of the reproductive numbers and clinical reporting (Table 2).

Using our expression of the reproductive number (2), the reproductive number for the fall wave $\hat{\mathscr{R}}_2=3.75$ (95% CI: 3.57–3.93) is significantly larger than that of the spring wave $\hat{\mathscr{R}}_1=1.49$ (95% CI: 1.45–1.53). This can be explained by the significantly higher estimate of the proportion of clinically ill cases during the second wave $\hat{\rho}_2=0.36$ (95% CI: 0.32–0.40) compared to our estimate of the first wave $\hat{\rho}_1=0.10$ (95% CI: 0.08–0.12) albeit our estimate of the transmission rate for the spring wave $\hat{\beta}_1=8$ (95% CI: 7.74–8.26) was slightly higher than our estimate for the fall wave $\hat{\beta}_2=5.75$ (95% CI: 5.27–6.23). We also found that if we reduce the contact rate for hospitalized cases by 25%, the reproductive number for the fall wave is reduced from 3.75 to 3, or slightly less than 25%. If the contact rate for hospitalized cases is reduced by 75%, the reproductive number for the fall wave is further reduced to 1.6.

Using a simple expression for the proportion of reported clinical cases (3), we estimated a clinical reporting rate of 59.7% (95% CI: 55.7–63.7) for the first wave and 83% (95% CI: 79–87) for the second wave. The higher clinical reporting during the second wave also reflects the corresponding higher diagnostic rate (Table 1). The distribution of the reproductive numbers and clinical reporting for the first and second waves are displayed in Fig. 6.

The model estimates for the recovery rate for the spring wave $\hat{\gamma_{1_1}}=0.34$ (95% CI: 0.32–0.36) and fall wave $\hat{\gamma_{1_2}}=0.45$ (95% CI: 0.37–0.53) are very similar. The diagnostic rate during the fall wave $\hat{\alpha_2}=2.14$ (95% CI: 1.92–2.36) is significantly larger than that of the spring wave $\hat{\alpha_1}=0.51$ (0.43–0.59) even though the variance of the estimate for the fall wave is significantly larger. In agreement with empirical data, our estimate of the mortality rate for the second wave $\hat{\delta}_2=0.02$ (95% CI: 0.016–0.024) is larger than our estimate for the spring wave $\hat{\delta}_1=0.008$ (95% CI: 0.004–0.012).

Our model predicts that the relative infectiousness of asymptomatic individuals q_i is quite small. Moreover, the distribution of q_i obtained from our simulation study is skewed to the right compared to the almost symmetric distributions of the rest of the parameter estimates (Fig. 5).

To support our estimates of the parameters β_i, γ_{1_i}, α_i, q_i, and ρ_i obtained through least-squares fitting, we evaluated the identifiability of the estimated model parameters by simulating 1000 alternate realizations of the epidemic curve. Our simulation study results (Fig. 5) confirm the stability of our parameter estimates to perturbations around the model output.

We assessed the effects of two types of interventions on the reproductive number of the fall wave by reducing the transmission rate (via parameter p) or the transmissibility of hospitalized individuals through effective isolation measures (via parameter ℓ). Our predictions for the effectiveness of interventions depend on the fitted parameter values. This implies that the uncertainty in these estimates translates into an uncertainty for our predictions, which we can quantify via a simulation study using the parametric bootstrap. Our results indicate that control can be achieved with certainty (probability 1) when the reduction in the transmission rate is $>76.5\%$. On the other

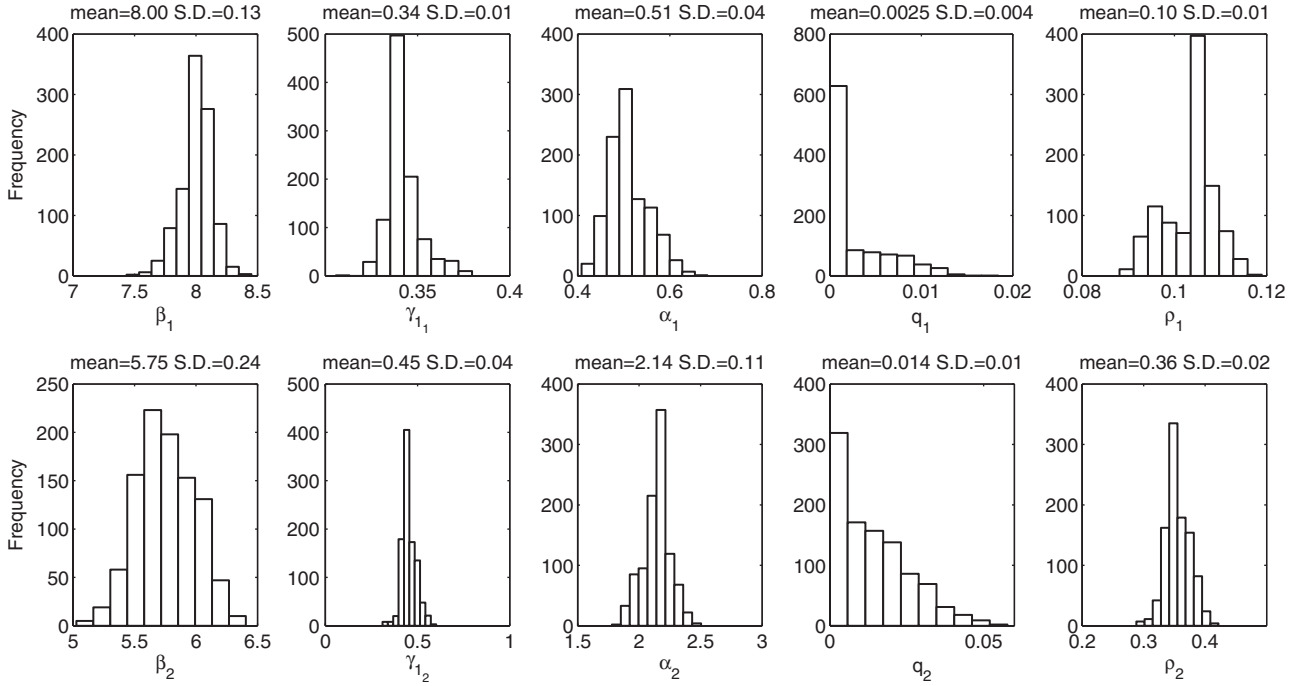

Fig. 5. The distribution of the parameter estimates obtained from our simulation study. The best fit of the cumulative number of reported cases $C(t, \hat{\mathbf{\Theta}}_i)$ to the data was perturbed by simulating alternate realizations. To the best-fit curve $C(t, \hat{\mathbf{\Theta}}_i)$ was added a simulated error structure computed using the increment in the "true" $C(t, \hat{\mathbf{\Theta}}_i)$ from day j to day $j+1$ as the Poisson mean for the number of new case notifications observed in the j to $j+1$ interval. Next, parameters were estimated (see parameter estimation). Results are shown for 1000 simulated realizations.

Table 2
Population parameters and estimated reproductive numbers and reporting rates for the spring and fall waves of the 1918/9 influenza pandemic in Geneva, Switzerland

Flu wave	Case fatality rate (%)	$\mathscr{R}$	S.D. $\mathscr{R}$	Reporting (%)	S.D. Reporting (%)
Spring	0.7 (Gani et al., 2005)	1.49	0.02	59.7	2.0
Fall	3.25 (Gani et al., 2005)	3.75	0.09	83.0	2.0

Estimates of the standard deviation (S.D.) for $\mathscr{R}_i$ and clinical reporting were obtained from our simulation study consisting of 1000 replicates (see Fig. 6).

hand, a reduction in the transmissibility of hospitalized individuals cannot guarantee control (or $\hat{\mathscr{R}}_c < 1$) with certainty. Our model predicts that effective isolation measures alone at its best (ℓ close to 0) would only guarantee control with probability 0.87. These observations can be readily seen in Fig. 7 showing the estimate of the reproductive number for the second wave subject to interventions $\hat{\mathscr{R}}_c$ and the probability of $\hat{\mathscr{R}}_c < 1$ as a function of each type of interventions alone. When both types of interventions are implemented simultaneously, achieving control is more feasible as can be seen in Fig. 8.

5. Discussion

In the context of influenza, mathematical models have been used to study different demographic and epidemiological mechanisms that characterize influenza dynamics such as annual periodicity (e.g. Castillo-Chavez et al., 1989; Boni et al., 2004; Nuño et al., 2005), describe and predict its spread (Elvebaek et al., 1976; Spicer and Lawrence, 1984; Rvachev and Longini, 1985; Flahault et al., 1988; Viboud et al., 2003; Hyman and Laforce, 2003), and evaluate different control strategies that could aid in the elaboration of preparedness plans against pandemics or bioterrorist attacks (Longini et al., 2005, 2004; Gani et al., 2005; Ferguson et al., 2005).

We have used a compartmental epidemic model with homogeneous mixing to describe the transmission dynamics during the spring and fall waves of infection of the 1918 influenza pandemic in the Canton of Geneva, Switzerland. The homogeneous mixing assumption implies that each individual has the same probability of contacting any of the other individuals in the population. In reality each individual interacts with a smaller group of individuals (Keeling and Grenfell, 2000). Thus, this assumption could bias our estimate of the transmission rate.

Our model retains the minimal complexity necessary to estimate model parameters and address specific public health questions. More detailed heterogeneity of the

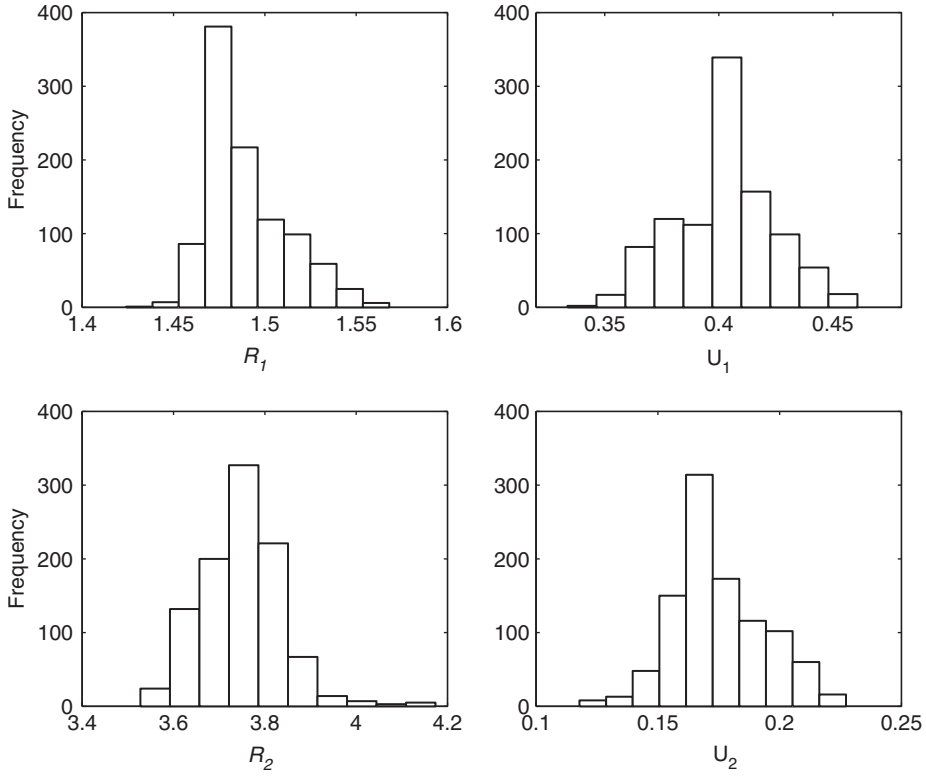

Fig. 6. The distribution of the reproductive number $\mathscr{R}_i$ and clinical underreporting U_i for the spring and fall waves of infection obtained by evaluating each set of parameter estimates (obtained from our simulation study of 1000 replicates) into formulas (2) and (4), respectively.

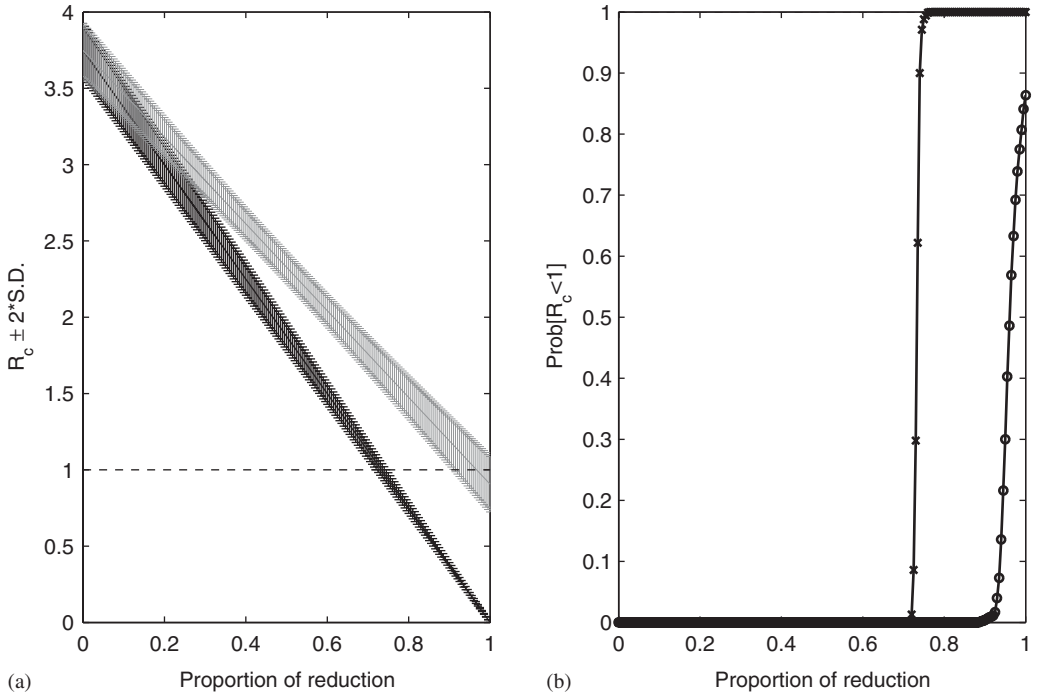

Fig. 7. The effects of two types of interventions on the reproductive number of the second wave and the probability of $\hat{\mathscr{R}}_c < 1$. (a) The reproductive number as a function of the effectiveness of isolation $(1-\ell)$ in hospitals (gray) and as a function of the proportion of reduction $(1-p)$ on the probability of transmission per contact (black). The solid line is the mean and the error bars represent the 95% confidence region around the mean using our 1000 realizations from our simulation study. The dashed line shows the epidemic threshold $\hat{\mathscr{R}}_c = 1$. (b) Control can be achieved with certainty when the reduction in the transmissibility per contact is $>76.5\%$ (cross). On the other hand, a reduction in the transmissibility of hospitalized individuals can only ensure control with probability 0.85 when "perfect" isolation measures are implemented (circles).

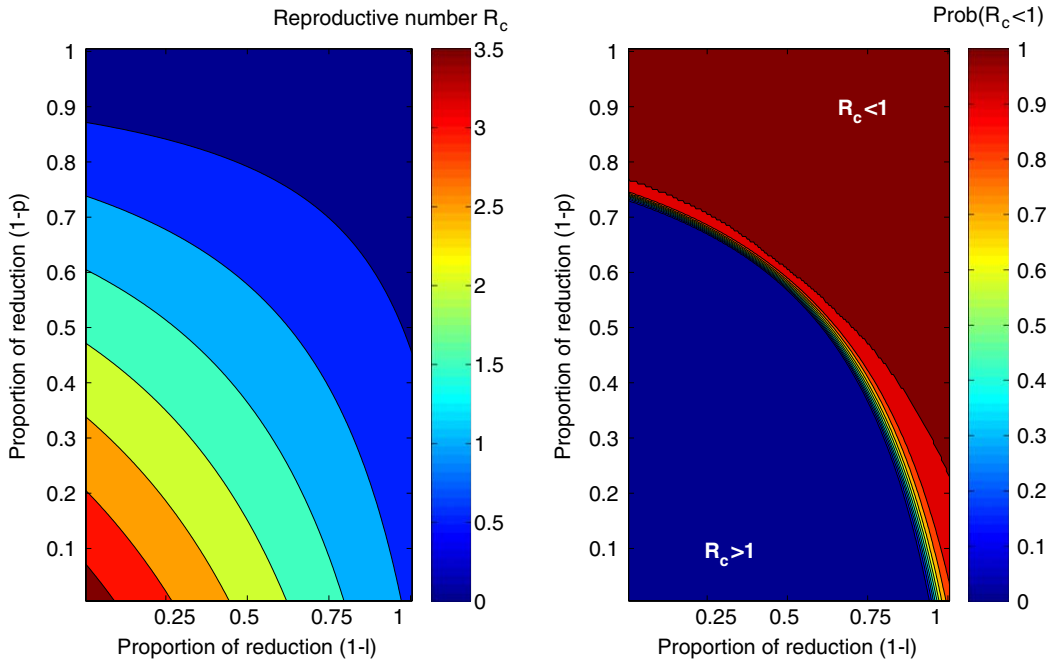

Fig. 8. The reproductive number $\hat{\mathscr{R}}_c$ for the second influenza wave (left) and the probability boundary level curves for $\hat{\mathscr{R}}_c = 1$ (right) as a function of the combined effect of two types of interventions namely the effectiveness of isolation $(1-\ell)$ and the reduction $(1-p)$ on the probability of transmission per contact.

population (i.e. susceptibility, infectiousness, and mortality according to age) would increase the model complexity and require more data to estimate the additional parameters.

Our model considers the possibility of limited transmission from subclinical cases, and the role of underreporting due to clinical cases that recover without being properly diagnosed in hospital clinics. For each wave, the transmission rate, the recovery rate, the diagnostic rate, the relative infectiousness of asymptomatic cases, and the proportion of clinical cases were estimated using least squares and the variance of the estimates were calculated from a simulation study. Estimates of the reproductive numbers and clinical reporting rates were obtained using expressions derived from the model structure. Even with the simplifying assumptions on mixing and population heterogeneity, our model was able to describe well the influenza waves of the Spanish flu epidemic in Geneva, Switzerland (Fig. 4) and supplied with reasonable parameter estimates.

Our models predicts a reduction in the transmission rate during the second wave (Table 1) which can be explained as the result of behavior changes in the population (see Del Valle et al., 2005) reducing the contact rate, reduced susceptibility of the general population (e.g. through increase hygienic practices, use of face masks), and sick individuals taking precautions to avoid infecting others.

Our estimate of the basic reproductive number for the first wave is similar to the baseline basic reproductive number of 1.39 reported by Gani et al. (2005) assuming a clinical attack rate of 25% and a serologic attack rate of 50%. Our estimate of the reproductive number for the second wave was significantly larger than that of the first wave and is above previous estimates for SARS (Chowell et al., 2003, 2004; Lipsitch et al., 2003; Riley et al., 2003). This is in agreement with the high severity of symptoms characteristic of the second wave (Ammon, 2001). This can be attributed partially from our $\mathscr{R}_i$ formula by the higher proportion of clinical cases estimated during the second wave (Table 1). These estimates can be compared with other estimates of the reproductive number obtained using mortality data (Mills et al., 2004; Gani et al., 2005). Mills et al. (2004) estimated the reproductive number to be in the range 2–3 using mortality data of the 1918 flu pandemic in the United States. Gani et al. (2005) estimated a reproductive number of 2 for the first wave and 1.55 for the second wave of the 1918 flu pandemic in UK.

A sensitivity analysis on the natural birth and death rate μ and the flu-specific mortality rates δ_i showed that our estimates of $\mathscr{R}_i$ are not significantly affected to small variations in these parameters. Furthermore, the general risk of death is known to vary with age, as did morbidity and mortality from the Spanish flu (Ammon, 2002). While the age-specific general mortality pattern is highest for infants and elderly, the age-specific influenza mortality was highest in the age group between 20 and 49 years (Ammon, 2002). A previous study based on an SEIR model concluded that estimates of the reproductive number were not affected due to age-specific transmission rates and case-fatality proportions (Mills et al., 2004). Differences in morbidity and mortality rates need to be incorporated in age-structured models that address questions regarding age-specific groups such as targeted control interventions (Longini et al., 2004).

Our model predicts that 40% of the clinical cases were not reported in hospitals during the first wave. This underreporting was reduced to 18% during the second wave. This can be explained by the high severity of symptoms and deadly complications experienced during the second wave of infection (Ammon, 2001) and the increasing awareness among the population about the ongoing epidemic.

We found that containment is possible through either the implementation of effective isolation strategies in hospital settings or reductions in the transmission rate. While "perfect" isolation of hospitalized cases only assures $\hat{\mathcal{R}}_c < 1$ with probability 0.87, reductions $> 76.5\%$ in the transmission rate of the general population can guarantee control. When both types of interventions are combined, their effect is nonlinear with the threshold condition for control $\hat{\mathcal{R}}_c < 1$ (Fig. 8), which facilitates control.

There is evidence of early herald waves of influenza in 1916 prior to the 1918/9 pandemic characterized by high mortality in the young (Oxford et al., 2001). The first wave of infection for the situation in Geneva, Switzerland seems to resemble the dynamics of annual outbreaks of influenza as indicated by its small basic reproductive number (Table 2). Today, the identification of these "early" outbreaks could give us more time to prepare for the coming pandemic by increasing the stockpiles of antivirals and possibly the preparation of new vaccines. This highlights the importance of maintaining global virological surveillance for influenza viruses to obtain information about future pandemic viruses that could aid in the elaboration of new vaccines (Kida et al., 2001). Rapid identification of emerging viruses can extend the time available from the appearance of the "early" herald waves to the actual pandemic waves. This is increasingly important and challenging because of our expanding highly interconnected worldwide transportation networks.

Acknowledgements

We thank two reviewers for providing useful comments that helped improve our manuscript. G. Chowell was supported by a Director's Postdoctoral Fellowship from Los Alamos National Laboratory.

References

Ammon, C.E., 2001. The 1918 Spanish flu epidemic in Geneva, Switzerland. Int. Congr. Ser. 1219, 163–168.

Ammon, C.E., 2002. Spanish flu epidemic in 1918 in Geneva, Switzerland. Eur Surveill 7, 190–192.

Anderson, R.M., May, R.M., 1991. Infectious Diseases of Humans. Oxford University Press, Oxford.

Boni, M.F., Gog, J.R., Andreasen, V., Christiansen, F.B., 2004. Influenza drift and epidemic size: the race between generating and escaping immunity. Theor. Popul. Biol. 65, 179–191.

Brauer, F., Castillo-Chavez, C., 2000. Mathematical Models in Population Biology and Epidemiology. Springer, New York.

Castillo-Chavez, C., Hethcote, H.W., Andreasen, V., Levin, S.A., Liu, W.M., 1989. Epidemiological models with age-structure, proportionate mixing, and cross-immunity. J. Math. Biol. 27, 233–258.

Chowell, G., Fenimore, P.W., Castillo-Garsow, M.A., Castillo-Chavez, C., 2003. SARS outbreaks in Ontario, Hong Kong and Singapore: the role of diagnosis and isolation as a control mechanism. J. Theor. Biol. 24, 1–8.

Chowell, G., Castillo-Chavez, C., Fenimore, P.W., Kribs-Zaleta, C., Arriola, L., Hyman, J.M., 2004. Model parameters and outbreak control for SARS. Emerg. Infect. Dis. 10, 1258–1263.

Cunha, B.A., 2004. Influenza: historical aspects of epidemics and pandemics. Infect. Dis. Clin. North Am. 18, 141–155.

Del Valle, S., Hethcote, H., Hyman, M., Castillo-Chavez, C., 2005. Effects of behavioral changes in a smallpox attack model. Math. Biosci. 195, 228–251.

Diekmann, O., Heesterbeek, J., 2000. Mathematical Epidemiology of Infectious Diseases: Model Building, Analysis and Interpretation. Wiley, New York.

Dubois, J., 2005. E-mail Communication. Office Cantonal de la Statistique—Geneve.

Efron, B., Tibshirani, R., 1986. Bootstrap methods for standard errors, confidence intervals, and other measures of statistical accuracy. Stat. Sci. 1, 54–75.

Elvebaek, L.R., Fox, J.P., Ackerman, E., Langworth, A., Boyd, M., Gatewood, L., 1976. An influenza simulation model for immunisation studies. Am. J. Epidemiol. 103, 152–165.

Enserink, M., 2005. Pandemic influenza: global update. Science 309, 370–371.

Ferguson, N.M., Cummings, D.A.T., Cauchemez, S., Fraser, C., Riley, S., Meeyai, A., Lamsirithaworn, S., Burke, D.S., 2005. Strategies for containing an emerging influenza pandemic in southeast Asia. Nature 437, 209–214.

Flahault, A., Letrait, S., Blin, P., Hazout, S., Menares, J., Valleron, J., 1988. Modelling the 1985 influenza epidemic in France. Stat. Med. 7, 1147–1155.

Gani, R., Hughes, H., Fleming, D., Griffin, T., Medlock, J., Leach, S., 2005. Potential impact of antiviral use during influenza pandemic. Emerg. Infect. Dis. 11, 1355–1362 Available from http://www.cdc.gov/ncidod/EID/vol11no09/04-1344.htm.

Hyman, J.M., Laforce, T., 2003. Modeling the spread of influenza among cities. In: Banks, T., Castillo-Chavez, C. (Eds.), Bioterrorism: Mathematical and Modeling Approaches in Homeland Security. SIAM's Series Frontiers in Applied Mathematics.

Johnson, N.P., Mueller, J., 2002. Updating the accounts: global mortality of the 1918–1920 "Spanish" influenza pandemic. Bull. Hist. Med. 76, 105–115.

Keeling, M.J., Grenfell, B.T., 2000. Individual-based perspectives on R_0. J. Theor. Biol. 203, 51–61.

Kida, H., Okazadi, K., Takada, A., Ozaki, H., Tashiro, M., Lvov, D.K., Shortridge, K.F., Webster, R.G., 2001. Global surveillance of animal influenza for the control of future pandemics. Int. Congr. Ser. 1219, 169–171.

Lipsitch, M., Cohen, T., Cooper, B., Robins, J.M., Ma, S., James, L., Gopalakrishna, G., Chew, S.K., Tan, C.C., Samore, M.H., Fisman, D., Murray, M., 2003. Transmission dynamics and control of severe acute respiratory syndrome. Science 300, 1966–1970.

Longini Jr., I.M., Halloran, M.E., Nizam, A., Yang, Y., 2004. Containing pandemic influenza with antiviral agents. Am. J. Epidemiol. 159 (7), 623–633.

Longini Jr., I.M., Nizam, A., Shufu, X., Ungchusak, K., Hanshaoworakul, W., Cummings, D.A.T., Halloran, M.E., 2005. Containing pandemic influenza at the source. Science 309, 1083–1087.

Meltzer, M.I., Cox, N.J., Fukuda, K., 1999. The economic impact of pandemic influenza in the United States: priorities for intervention. Emerg. Inf. Dis. 5, 659–671.

Mills, C.E., Robins, J.M., Lipsitch, M., 2004. Transmissibility of 1918 pandemic influenza. Nature 432, 904–906.

Moritz, A.J., Kunz, C., Hofman, H., Liehl, E., Reeve, P., Maassab, H.F., 1980. Studies with a cold-recombinant A/Victoria/3/75 (H3N2) virus, II: evaluation in adult volunteers. J. Infect. Dis. 142, 857–860.

Neter, J., Wasserman, W., 1974. Applied Linear Statistical Models. Richard D. Irwin, Inc., Homewood, IL.

Nuño, M., Feng, Z., Martcheva, M., Castillo-Chavez, C., 2005. Dynamics of two-strain influenza with isolation and partial cross-immunity. SIAM J. Appl. Math. 65, 3, 964–982.

Oxford, J.S., Sefton, A., Jackson, R., Innes, W., Daniels, R.S., Johnson, N.P.A.S., 2001. Early herald wave outbreaks of influenza in 1916 prior to the pandemic of 1918. Int. Congr. Ser. 1219, 155–161.

Patterson, K.D., Pyle, G.F., 1991. The geography and mortality of the 1918 influenza pandemic. Bull. Hist. Med. 65, 4–21.

Pillonetto, G., Sparacino, G., Cobelli, C., 2003. Numerical non-identifiability regions of the minimal model of glucose kinetics: superiority of Bayesian estimation. Math. Biosci. 184, 53–67.

Pourbohloul, B., Ancel Meyers, L., Skowronski, D.M., Krajden, M., Patrick, D.M., Brunham, R.C., 2005. Modeling control strategies of respiratory pathogens. Emerg. Infect. Dis. 11, 1249–1255.

Reeve, P., Gerendas, A.B., Moritz, A., Lihel, E., Kunz, C., Hofman, H., Maassab, H.F., 1980. Studies in man with cold-recombinant influenza virus (H1N1) live vaccines. J. Med. Virol. 6, 75–83.

Riley, S., Fraser, C., Donnelly, C.A., Ghani, A.C., Abu-Raddad, L.J., Hedley, A.J., Leung, G.M., Ho, L.M., Lam, T.H., Thach, T.Q., Chau, P., Chan, K.P., Lo, S.V., Leung, P.Y., Tsang, T., Ho, W., Lee, K.H., Lau, E.M., Ferguson, N.M., Anderson, R.M., 2003. Transmission dynamics of the etiological agent of SARS in Hong Kong: impact of public health interventions. Science 300, 1961–1966.

Robine, J.M., Paccaud, F., 2005. Nonagenarians and centenarians in Switzerland, 1860–2001: a demographic analysis. J. Epidemiol. Community Health 59 (1), 31–37.

Rvachev, L.A., Longini Jr., I.M., 1985. A mathematical model for the global spread of influenza. Math. Biosci. 75, 3–22.

Snacken, R., 2002. Pandemic planning. Vaccine 20, S88–S90.

Spicer, C.C., Lawrence, C.J., 1984. Epidemic influenza in greater London. J. Hyg. (London) 93, 105–112.

Viboud, C., Boelle, P.Y., Carrat, F., Valleron, A.J., Flahault, A., 2003. Prediction of the spread of influenza epidemics by the method of analogues. Am. J. Epidemiol. 158 (10), 996–1006.

Webby, R.J., Webster, R.G., 2003. Are we ready for pandemic influenza? Science 302, 1519–1522.

Webster, R.G., Bean, W.J., Gorman, O.T., Chambers, T.M., Kawaoka, Y., 1992. Evolution and ecology of influenza A viruses. Microbiol. Rev. 56, 152–179.